



Convective Heat Transfer of Spring Meltwater Accelerates Active Layer Phase Change in Tibetan Permafrost Areas

Yi Zhao¹, Zhuotong Nan^{1,2*}, Hailong Ji¹, Lin Zhao³

5 ¹Key Laboratory of Ministry of Education on Virtual Geographic Environment, Nanjing Normal University, Nanjing, 210023, China

²Jiangsu Center for Collaborative Innovation in Geographical Information Resource Development and Application, Nanjing, 210023, China

³School of Geographical Sciences, Nanjing University of Information Science & Technology, Nanjing
10 210044, China

Corresponding author: Zhuotong Nan (nanzt@njnu.edu.cn)



Abstract.

Convective heat transfer (CHT) is one of the important processes that controls the near ground surface
15 heat transfer in permafrost areas. However, this process has often not been considered in most permafrost
simulation studies and its influence on the freeze-thaw processes of the active layer lacks quantitative
investigation. The Simultaneous Heat and Water (SHAW) model is one of the few land surface models
in which the CHT process is well incorporated in the soil heat-mass transport processes. We applied the
SHAW model to investigate the impacts of CHT on active layer thermal dynamics on the Tanggula
20 station, a typical permafrost site located at the eastern Qinghai-Tibetan Plateau with abundant
meteorological and soil temperature/moisture observation data. The 2008-2009 observed hourly data
were used to calibrate the model parameters and those of 2010 for validation. A control experiment was
carried out to quantify the changes in active layer thermal regime affected by vertical advection of liquid
water, consisting of three setups: using (1) the original SHAW model with full consideration of CHT; (2)
25 a modified SHAW model ignoring the CHT due to infiltration from the surface, and (3) a modified
SHAW model ignoring complete CHT processes in the system. The impacts of vapor convection are not
considered in this experiment. The results show that the CHT events mainly happened during thawing
periods when the active layer melted at shallow (0-0.2m) and middle (0.4-1.3 m) soil depths, and its
impact on soil thermal regime at shallow depths was significantly greater in spring melting periods than
30 in summer. The impact was minimal in freezing periods and in deep soil layers. During melting periods,
temperatures in the shallow and middle soil depths simulated under the scenario considering CHT were
higher by up to 10.0 and 1.5 °C, respectively, than those under the scenarios ignoring CHT. The ending
dates of zero-curtain effect were considerably advanced with CHT considered, due to the warming effect
of CHT associated with infiltration. However, the opposite cooling effect also existed due to presence of
35 upward liquid fluxes and thermal differences between the soil layers. In some certain period, the
advection flow including partial return flow reduced the temperatures in the shallow and middle depths
by as much as -5.0 and -1.0 °C, respectively. The overall annual effect of CHT by liquid flux is to increase
soil temperature in the active layer and favors thawing of frozen ground at the study site.

Keywords: convective heat transfer, active layer, permafrost, hydrological and thermal processes,
40 Simultaneous Heat and Water (SHAW) Model



1. Introduction

Permafrost is defined as the ground that continuously remains frozen for longer than two years (Zhao et al., 2010), and is mainly distributed at the high latitudes and cold alpine areas, such as Antarctic, Arctic and Qinghai-Tibet Plateau (QTP) (Zhang et al., 1999). Given the currently warming trends in much of the permafrost areas of the Earth (Biskaborn et al., 2019), significant changes in permafrost dynamics are likely to occur and the local ecosystem and environment have already been seriously influenced (Cheng and Wu, 2007; Jin et al., 2009; Jorgenson et al., 2001; Tesi et al., 2016). It is thus very important to accurately understand soil thermal and hydrological processes occurring in frozen ground regions.

It is usually recognized that ground thermal transfer is more than a single heat conduction process controlled by the upper and lower boundary conditions, but should be a complex system that considers both conductive and non-conductive heat transfer (Kane et al., 2001; Putkonen, 1998). Nonconductive heat processes refer to all those heat transfer processes that can significantly impact the thermal regime but not explicitly described by heat conduction theory, including: (1) latent heat exchange; (2) vapor convective heat transfer (CHT) caused by vapor pressure gradient or thermal gradient (Cahill and Parlange, 1998); (3) CHT due to infiltration of meltwater and rainwater from surface and due to advection within the soils (Scherler et al., 2011; Woo et al., 2000). Despite the predominance of thermal conduction in permafrost regions, the role of non-conductive processes on active layer freeze-thaw cycles cannot be ignored (Boike et al., 2008). Due to temperature and pressure differences, vapor heat flows from a warm layer to a cold layer and it cools soil temperature in the upper layers if the upward gradients are present (Cahill and Parlange, 1998; Halliwell and Rouse, 1987). Evaporation also has the same effect in cooling soils due to the loss of heat from the soils (Roth and Boike, 2001; Shen et al., 2015). These cooling effects of vapor transport have been applied to protect engineering infrastructures from frost heave hazards in permafrost regions (Cheng, 2004; Cheng et al., 2008). Liquid water migration can be usually forced by gravitational, pressure or osmotic pressure gradients in the soils during the thawing periods. Rapid temperature increases are often observed in the upmost soil layer during the snow melts in spring and summer rain falls, indicative of warming effects of liquid CHT (Hinkel et al., 1997; Kane et al., 1991). In the freezing period, because the freezing process occurring in the active layer increases the pore fluid density and van der Waals forces on the ice particles surface, the residual water convection could ensue and CHT of liquid water is relatively modest but still work (Fisher et al., 2020; Kane and Stein, 1983).



Understanding the impacts of CHT on frozen ground is important for accurately simulating ground temperature and concomitant hydrology in permafrost regions in the context of global climate warming. However, although some convective heat effects have been observed, they are often produced by simultaneous processes such as heat conduction, advection and convection, and phase change. The in situ instrumentation is still limited to accurately measure key soil thermal and hydrological variables. It is challenged to isolate the sole impacts of CHT from the totality of soil heat transfer processes (Hasler et al., 2008; Pogliotti et al., 2008).

Physically explicit numerical models are effective tools for isolating the impact of a single process from the overall system. These models could provide information that is otherwise impossible by observation techniques. Most existing land surface models such as Noah and Community Land Model (CLM), despite extensive use in modelling cold region processes (Gao et al., 2019; Guo and Wang, 2013; van der Velde et al., 2009; Wu et al., 2018), implement only heat conduction (Zhang et al., 2008) and phase change (Qi et al., 2013; Riseborough, 1990) in energy balance. The neglect of CHT mechanism in these models generally leads to increased uncertainty due to deficiency in physics. Thus, a number of soil thermal and hydrological processes simulation tools that specifically take into account CHT have been developed. Luethi et al. (2017) estimated the heat transfer efficiency of vapor and liquid convection. Hansson et al. (2004) presented a fully implicit numerical model for coupled heat transport and variably saturated water flow. Wicky et al. (2017) developed a numerical model considering air flow in permafrost talus slopes, and revealed distinct seasonality of air flow cycle on talus slopes and considerable seasonal differences in terms of the impacts on soil temperature. Orgogozo et al. (2019) and Kurylyk et al. (2016) have, respectively, established three-dimensional coupled soil heat and water models to explore the effects of soil evapotranspiration and runoff on soil temperature. While their studies improve our understanding on the role of CHT in altering permafrost thermal dynamics, they focused on region-specific permafrost conditions and the established methodologies were hard to be transferred to other regions with conditions dissimilar to those study regions.

The Simultaneous Heat and Water (SHAW) model is one of the well-known one-dimensional coupled hydraulic-thermal models that integrates mass and energy transfer processes of the atmosphere-vegetation-soil continuum into a simultaneous solution (Flerchinger and Saxton, 1989a). This model considers detailed physics of interrelated mass and energy transfer mechanisms including precise



100 convective heat transport processes of liquid water and vapor, which makes it outperform the peer LSMs
in simulating the active layer freezing-thawing processes in permafrost regions. The SHAW model has
many applications in permafrost regions, including investigating responses of frozen ground to climate
and land use change (Huang and Gallichand, 2006; Zuo et al., 2019), interaction of ground water and
active layer (Chen et al., 2019; Cui et al., 2020), and energy/mass exchange at the surface-atmosphere
105 interface (Kahimba et al., 2009). Previous studies has indicate good accuracy of SHAW in simulating
the dynamics of soil temperature, moisture (Flerchinger and Pierson, 1997) and the freezing-thawing
cycle (Flerchinger and Saxton, 1989b) repeatedly occurring in the active layer.

Therefore, this study utilizes the SHAW model to quantify the impacts of liquid CHT on the active layer
temperature and moisture content through numerical modeling at a typical permafrost distributed area
110 site, i.e., the Tanggula (TGL) site, on the QTP, China. The SHAW model was modified to remove the
CHT processes and control experiments were subsequently set up to simulate comparative scenarios with
or without considering CHT in the model. The objectives are: (1) to demonstrate temporal and depth
characteristics of the CHT events; (2) to quantify the impacts of liquid CHT on the thermal regime of
active layer; (3) to elucidate the interplay of heat and soil moisture in the freezing-thawing process
115 occurring in the active layer.

2. Methods and Data

2.1 The Simultaneous Heat and Water model

The SHAW model is one of the well-known vertical one-dimensional thermal and hydrological migration
coupling models (Flerchinger and Saxton, 1989a, 1989b). It has been widely used to simulate heat, water
120 and solute flux exchange processes between vegetation canopy, snow cover, soil residue layer and the
soil layer. In addition to the conductive heat transfer and phase change process, the SHAW model also
considers the heat transfer associated with the advection and convection of vapor and liquid water in its
energy balance equation, which makes it outperforms the other land surface models such as Noah LSM
and CLM in simulating active-layer thermal regime. The SHAW model has proven itself as an effective
125 tool to simulate, to name a few, the permafrost evolution(Wei et al., 2011), the characteristics of freeze-



thaw cycle (Chen et al., 2019; Cui et al., 2020), and the land ecosystem changes (Flerchinger et al., 1996; Kahimba et al., 2009; Link et al., 2004).

For each soil layer stratified for the SHAW model, the net energy budget is equal to the sum of conductive heat flux, the CHT from liquid and vapor migration, the latent heat of water phase change and the change
130 of temperature. The one-dimensional energy balance equation for each layer is:

$$\frac{\partial}{\partial z} \left(k_s \frac{\partial T}{\partial z} \right) - \rho_l c_l \frac{\partial (q_l T)}{\partial z} - L_v \left(\frac{\partial \rho_v}{\partial t} + \frac{\partial q_v}{\partial z} \right) = C_s \frac{\partial T}{\partial t} - \rho_i L_f \frac{\partial \theta_i}{\partial t} \quad (1)$$

where C_s is the effective volumetric heat capacity of the soil layer ($\text{J}\cdot\text{m}^{-3}\cdot\text{C}^{-1}$) representing a lumped influence of minerals, liquid, ice and vapor in the soil layer; T is the soil temperature in this layer ($^{\circ}\text{C}$); ρ_i , ρ_l , ρ_v are the densities of ice, liquid water and vapor ($\text{kg}\cdot\text{m}^{-3}$), respectively; L_f and L_v are the latent
135 heats of fusion and vaporization ($\text{kJ}\cdot\text{kg}^{-1}$), respectively; θ_i is the volumetric ice content of the soil layer ($\text{m}^3\cdot\text{m}^{-3}$); q_l and q_v are the liquid water flux ($\text{m}\cdot\text{s}^{-1}$) and vapor flux ($\text{kg}\cdot\text{m}^{-2}\cdot\text{s}^{-1}$), respectively; k_s is the soil thermal conductivity ($\text{W}\cdot\text{m}^{-1}\cdot\text{C}^{-1}$); c_l is the specific heat capacity of water ($\text{J}\cdot\text{kg}^{-1}\cdot\text{C}^{-1}$); t and z are the time step and the depth centered in the present layer. The second term on the left hand side of Eq. 1 represents the heat flux caused by the migration of liquid pore water. The soil moisture diffusion
140 equation of each layer is:

$$\frac{\partial}{\partial z} \left[K \left(\frac{\partial \psi}{\partial z} + 1 \right) \right] + \frac{1}{\rho_l} \frac{\partial q_v}{\partial z} + U = \frac{\partial \theta_i}{\partial t} + \frac{\rho_i}{\rho_l} \frac{\partial \theta_i}{\partial t} \quad (2)$$

where K is the hydraulic conductivity ($\text{m}\cdot\text{s}^{-1}$); ψ is the soil matric potential (m) and U is a source/sink term for water uptaken by roots ($\text{m}^3\cdot\text{m}^{-3}\cdot\text{s}^{-1}$).

The inputs of the SHAW model consist of three types of data: (1) meteorological driving data including
145 air temperature, relative humidity, wind speed, precipitation, density of new snow, and shortwave radiation; (2) soil moisture content and soil temperature data as initial states and lower boundary conditions; (3) characteristic parameters of canopy, snow, soil residue and soil column at the study site.

2.2 Design of the control experiment

The SHAW model incorporates the CHT processes of the liquid and vapor flux in the energy budget
150 equation, which makes it possible to portray complete water-heat interactions frequently occurring in the freezing and thawing periods in permafrost regions. In this study we designed a control experiment containing three scenarios for representing full presence, partial presence and complete absence of liquid CHT in the model by modifying the model codes. We used the same forcing data at a typical permafrost



155 site, the TGL, to drive the models. The impacts of liquid CHT on active layer dynamics are quantified
by the differences in soil temperature and moisture content by contrasting the results from the three
scenarios.

The control experiment consists of three scenarios:

1. Control: in this setup the original SHAW model is applied to the TGL site and the simulated
results serves as a baseline to contrast with the results of other scenarios. Confined within the
160 physical limits, the soil parameters associated with each layer were calibrated to best match the
observed soil temperatures and moisture contents at various depth, i.e., 0.05 m, 0.1 m, 0.4 m,
1.05 m and 2.45 m. The same calibrated soil parameter values are used in the other two scenarios
to maintain consistency throughout the experiment.
2. No surface CHT (NoSurf): CHT between the ground surface and the soil is not considered in
165 this setup. For this purpose, the codes related to liquid water CHT from the ground surface layer
to the top soil layer (0.00 m) as described in the second term on the left hand side of the Eq. 1
were disabled in the SHAW model. By contrasting the results of this setup with that of Control,
the effects of the infiltrative convective heat could be quantified.
3. No CHT (NoConv): This setup completely eliminates the liquid water CHT, that is, both the
170 infiltrative convection from the surface to the top soil and the heat transfer associated with the
liquid water migration within the soil layers are not considered. All codes related to the second
term on the left hand side of Eq. 1 were disabled. By contrasting Control-NoConv with Control-
NoSurf, the impacts of CHT relating to vertical advection within soil layers will be determined.

Note, in the NoSurf and NoConv setups, we only removed heat fluxes and the exchanges associated with
175 the water movement, and still retained liquid water fluxes that is necessary to maintain the water balance
in each soil layer. In the SHAW model, we found the simulated direction of vapor flux did not match the
real vapor cycle, so the vapor-related convection keeps intact in the three setups to exclude the impacts
of vapor CHT in this analysis. The three scenarios were simulated with the same upper/lower boundary
conditions, meteorological forcing data, initial states and calibrated parameters. Thus, the resultant
180 differences obtained between NoSurf/NoConv and Control simulations represent the impacts of liquid
CHT occurrences in discrete places. Greater simulated soil temperatures of Control than those of the



other two scenarios signify a positive thermal impact of CHT on the active layer, and it is a negative impact if they are lower.

2.3 Experimental area and data

185 A typical permafrost site, the TGL site, was chosen for the investigation due to its detailed observations of the active layer. The TGL site is situated on a southwest-facing slope elevated at 5100 m a.s.l. in the Tanggula mountains on the eastern QTP, with latitude 33°04' N and longitude 91°56' E. The local vegetation is sparse alpine meadow with a coverage fraction of about 30~40%. The soils are mainly composed by loamy sand (sand content > 70%). The annual mean of air temperature is about -4.9 °C. The
190 active-layer thickness (ALT) is measured as about 3 m (Xiao et al., 2013). The annual precipitation is about 400 mm and it mostly concentrates in the months from May to September, accounting for 92% of the whole year.

The installed instruments include an automatic weather station, which measures air temperature, wind speed and direction, humidity, shortwave/longwave radiation (upward and downward), air pressure,
195 snow depth, and precipitation, and an active-layer monitoring system, which measures soil temperatures and moisture contents at the depths of 0.05, 0.10, 0.20, 0.40, 0.70, 1.05, 1.30, 1.75, 2.10, 2.45 and 2.80 m below the surface. The time series of observed half-hourly air temperature, relative humidity, wind speed, precipitation and shortwave radiation from 2008 to 2010, collected from the automatic weather observation station measured at 2-m height at the TGL site, were used to drive the SHAW model running
200 at a time step of one hour. The observed daily soil temperature and unfrozen water content (UWC) at 0.05 m, 0.1 m, 0.4 m, 1.05 m and 2.45 m depth during the same period, collected from the active layer monitoring system, were used to calibrate and validate the SHAW model.

2.4 Model settings

Driving data. In addition to the hourly meteorological data from the TGL site, the inputs to the SHAW
205 model also include the snow density of each new snowfall event. We set them as zeros and let the model estimate it based on the air temperature at the time.

Soil column stratification. The soil column was stratified into 13 layers corresponding to the observation depths in the TGL site, including five layers (centered at 0.00, 0.02, 0.05, 0.1 and 0.2 m) as



the shallow depths, five layers (centered at 0.4, 0.5, 0.7, 1.05 and 1.3 m) as the middle depths and three
210 layers (centered at 1.75, 2.1 and 2.45 m) as the deep depths. The SHAW model requires a special layer
at the depth of zero as the interface between atmosphere, vegetation and soils. The shallow depths were
tightly discretized in order to accommodate rapid hourly variations in soil temperature and moisture near
the ground surface.

Boundary conditions. The SHAW model depends on accurate lower boundaries usually specified at a
215 shallow depth to enable a precise simulation of the coupled water-heat exchange processes (Chen et al.,
2019). In this study, the observations at the 2.8 m depth close to the active layer bottom were provided
as the lower boundaries. The observed daily soil temperatures at this depth constrain heat fluxes through
the lower boundary interface. The lower boundary of the soil moisture contents (both ice and unfrozen
water contents) was determined by the model following an empirical equation in relation to soil
220 temperature by confining the maxima of liquid water equivalent to $0.25 \text{ m}^3/\text{m}^3$ occurring in summer.

Initial conditions and spin up. For all the setups, initial soil temperature and soil moisture profiles were
generated with three decades' spinning up with repeating forcing data from 2008-2010, until the
differences in soil temperature and moisture content are narrowed to be less than $0.1 \text{ }^\circ\text{C}$ and $0.01 \text{ m}^3/\text{m}^3$,
respectively, between the last cycle and penultimate cycle at the same date for all soil layers. The eventual
225 soil temperature and moisture profiles were provided to each scenario simulation as the initial states.

Parametric calibration, model validation and simulation. According to a previous study at the same
TGL site (Liu et al., 2013) that suggests with the default parameter values the SHAW model simulated
well surface energy fluxes and soil temperatures, except for soil moisture content that was seriously
underestimated, we calibrated those hydraulic parameters in the model relating to soil moisture content
230 while maintaining the other parameters as their default values. The data from 2008-2009 were used for
calibration and 2010 for validation. The model was run on an hourly time step and the results were then
aggregated to a daily scale to ease the comparisons and analyses. The ranges of hydraulic parameter
values were roughly determined with reference to the previously studies (Chen et al., 2019; Wu et al.,
2018; Liu et al., 2013) and were then optimized for each soil layer by a process of trial and error. Two
235 metrics including the Nash-Sutcliffe efficiency coefficient (NSE) and root mean square error (RMSE)
were used to quantify the model performance:

$$\text{NSE} = 1 - \frac{\sum_{t=1}^N (O^t - M^t)^2}{\sum_{t=1}^N (O^t - \bar{O})^2} \quad (3)$$



$$\text{RMSE} = \sqrt{\frac{1}{N} \sum_{t=1}^N (O^t - M^t)^2} \quad (4)$$

where O^t and M^t are the observed value and simulated value in the time step t ; \bar{O} is the mean of the
 240 observations in the entire period; and N is the total number of time steps.

3. Results

3.1 Model evaluation

Table 1 shows the vertical discretization of the TGL soil profile and some of the important soil parameters
 associated with each layer. The volumetric percentages of sand, silt and clay and the bulk density were
 245 measured and the other four parameters, i.e., saturated hydraulic conductivity, air-entry potential,
 saturated volumetric moisture content, and pore-size distribution index, were obtained by calibration.

Table 1 Important soil parameter values for the TGL soil profile; ρ_b , the bulk density; K_s , the saturated hydraulic conductivity; ψ_e , air-entry potential, θ_s , saturated volumetric moisture content; b , pore-size distribution index.

Depth (m)	Sand (%)	Silt (%)	Clay (%)	ρ_b (g·cm ⁻³)	K_s (cm·h ⁻¹)	ψ_e (m)	θ_s (m ³ ·m ⁻³)	b
0	93	1	6	1176	25.5	-0.5	0.35	4.74
0.02	93	1	6	1176	25.5	-0.5	0.35	4.74
0.05	93	1	6	1176	25.5	-0.5	0.35	4.74
0.10	93	1	6	1176	25.5	-0.5	0.35	4.74
0.20	87	3	10	1331	25.5	-0.5	0.35	4.26
0.40	89	2	9	1103	25.5	-0.3	0.3	4.26
0.50	87	3	10	1105	25.5	-0.3	0.3	4.26
0.70	84	3	13	1405	20.05	-0.3	0.3	4.26
1.05	75	7	18	1235	20.05	-0.3	0.3	3.88
1.30	75	7	18	1281	20.05	-0.2	0.3	3.88
1.75	71	8	21	1253	20.05	-0.2	0.3	3.88
2.10	71	8	21	1460	20.05	-0.2	0.3	3.88
2.45	71	8	21	1248	20.05	-0.2	0.3	3.88



250

The SHAW simulations of soil temperature (left panels) and UWC (right panels) at the depths of 0.05 m, 0.1 m, 0.4 m, 1.05 m and 2.45m are presented in Figure 1. Overall, it confirms a good capability of the SHAW model in simulating the complex freezing and thawing processes in the active layer given reliable lower boundaries. The seasonal variations of both soil temperature and moisture in the TGL active layer were successfully captured. The simulated and observed soil temperatures were in particularly good agreement at the TGL site in both the calibration and validation periods. Specifically, the NSE values between the simulated and observed soil temperatures exceed 0.70 in most soil layers in either period, except the one at the depth of 1.05 m in the validation period, and are highest (up to 0.90) in the shallow layers. The RMSE values for the temperature decrease downward along with soil depth as the deep depths have smaller interannual fluctuations in temperature than the shallow depths. Despite relatively lower performance in UWC, the simulation of UWC still achieves NSE values exceeding 0.42 at all soil layers, and RMSE values of around $0.05 \text{ m}^3 \cdot \text{m}^{-3}$. We noticed abnormal abrupt declines of observed UWC at the 0.05 m and 0.1 m depths in summer of 2009 (Figure 1f, g), which were caused by equipment malfunction. Also, at the depths of 0.4 m and 1.05 m, some unrealistic zero observations of UWC were presented during the winter periods (Figure 1h, i). Many studies have already revealed a small amount of liquid pore water (ca. $0.05 \text{ m}^3 \cdot \text{m}^{-3}$) continues to exist even if the soil is completely frozen (Stein and Kane, 1983). Those abnormal zero values recorded are likely related to the inadequate capability of the time domain reflectometry sensors in detecting immobile residual liquid water. We believe in those periods the simulation results seem more realistic.

255

260

265

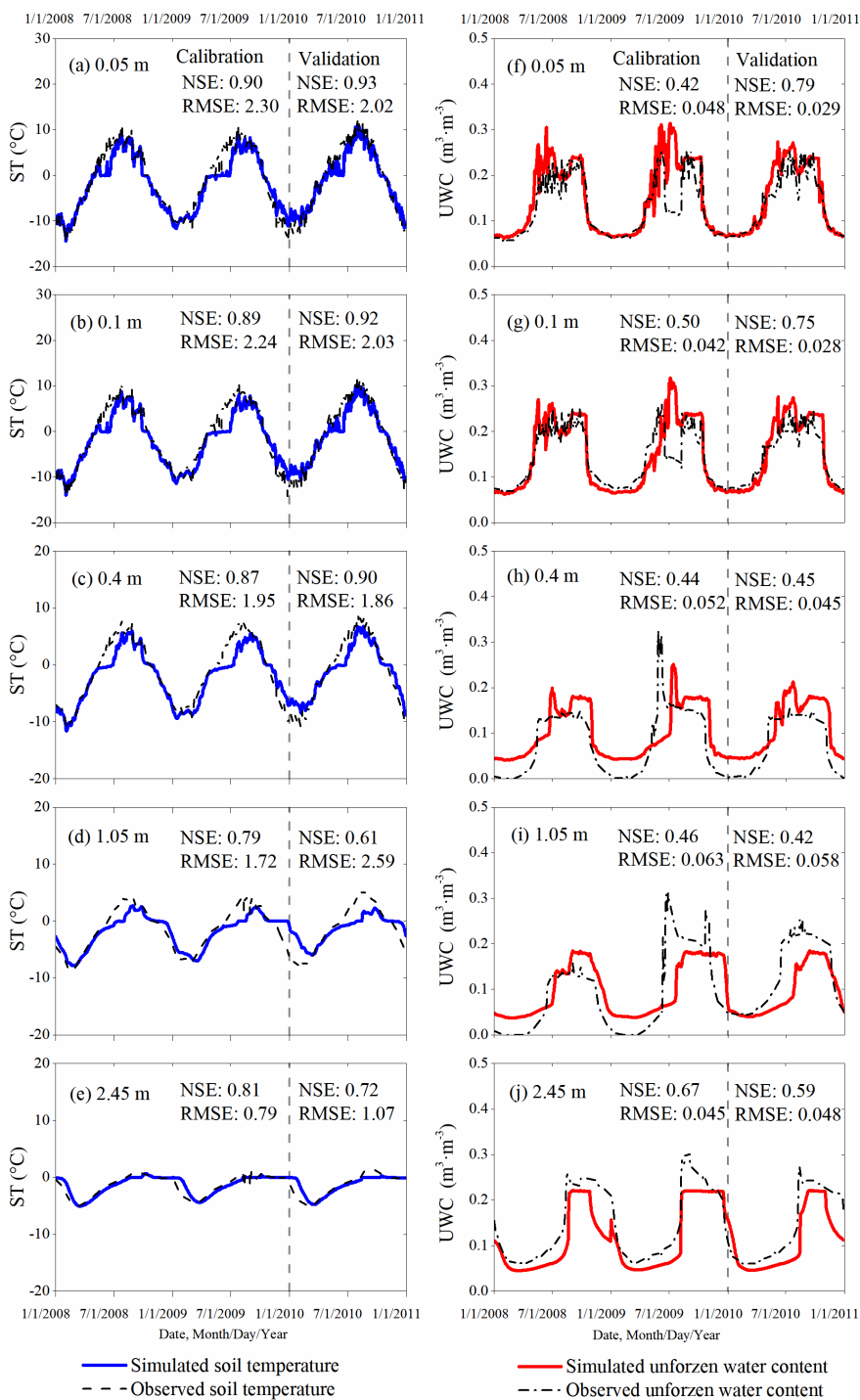




Figure 1 Simulated and observed daily soil temperatures (left panels) and unfrozen water contents (UWC; right panels) at the 0.05 m (a and f), 0.1 m (b and g), 0.4 m (c and h), 1.05 m (d and i) and 2.45m (e and j) depths at the Tanggula (TGL) site during 1 January 2008 to 31 December 2010.

During the thawing period in spring each year, the observed temperatures (Figure 1a-e) rapidly increased
275 from the negative to the positive, but the simulated soil temperatures exhibited an obvious, prolonged
duration of the zero-curtain effect, which delayed warming of soil temperature for days. The effect was
especially strong in 2009. The formation of zero-curtain is a joint result of multifaceted thermal processes
including evapotranspiration, phase change, thermal conduction and convection during the freezing and
thawing periods (Outcalt et al., 1990), and is more obvious during the thawing periods than freezing
280 periods (Jiang et al., 2018). The overestimation of the zero-curtain duration in the SHAW simulation is
primarily related to the irrational vapor movement and simplified ice-liquid phase change process.
In January 2010, overestimation of soil temperature was observed throughout the entire soil column
(Figure 1a-e). However, this phenomenon was not present in the same month in 2008 and 2009. It is
certain that the observed discrepancies result from unusually warm air temperature (Figure 2). These
285 anomalies also caused additional snowmelt events with ca. 0.5 mm of snow water equivalent in this
month (Figure 2).

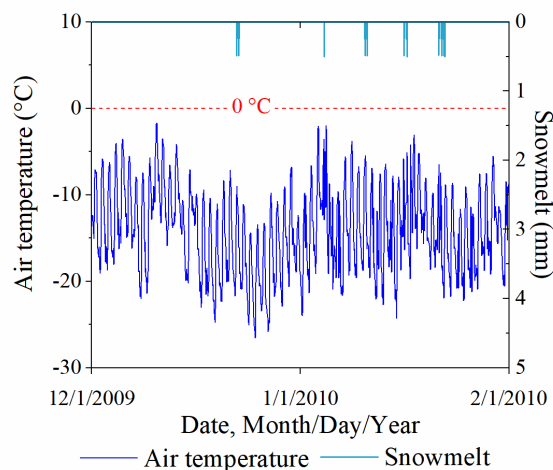


Figure 2 Unusual warm air temperature in January 2010 relating to the overestimation of modelled soil temperature in this month and the simulated hourly snow melt also impacted by the air temperature.



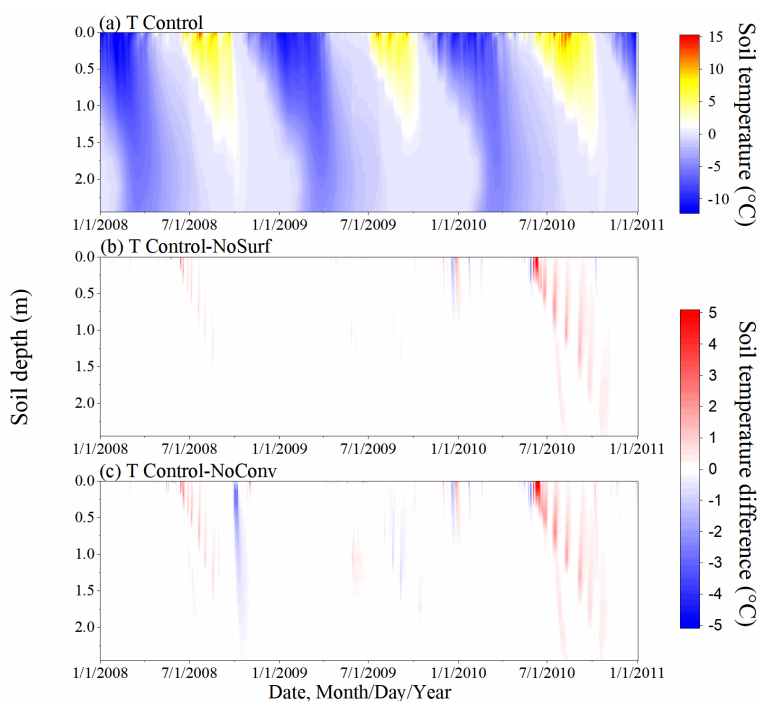
290 **3.2 General characteristics of convective heat transfer impacts**

The simulations of hourly soil temperature profiles under the Control scenario which uses the original SHAW model considering the full CHT processes are shown in Figure 3a. The effects of CHT appeared mainly in the thawing periods of 2008 and 2010, resulting in altering soil temperature profiles as shown in Figure 3b and c, which exhibit the differences in soil temperature between the Control and the two scenarios partially (NoSurf) or fully (NoConv) ignoring consideration of CHT in the model. However, 295 in the same periods of 2009, no noticeable temperature differences were simulated between Control and NoSurf for the entire soil column, and only slight differences between Control and NoConv in the middle depths. Because the vapor convection has not been modified, those effects solely come from the partial or full presence of CHT due to surface infiltration and vertical advection within the soil column. The soil 300 temperature differences were also noticeable at shallow depths in January 2010 (Figure 3b and c), when the soils at those depths were frozen. This phenomenon was in line with the occurrence of extra snowmelt events in this period as shown in Figure 2. It suggests that CHT could also take place in freezing periods provided that liquid pore water migrates in response to external air temperature changes in these periods. As shown in Figure 3b and c, the occurrence of CHT were more and more delayed with soil depth with 305 the most delayed taking the lowest place. The shallow depths are characterized with long thawing periods spanning from later spring to summer with large thermal gradients and active water migration between soil layers, so that CHT in those depths considerably impacts the thermal regime. Conversely, in deep depths where the temperature gradient and water motion are relatively modest, the thermal effects of CHT are much smaller. The differences between the Control and NoConv (Figure 3c) are more evident 310 than those between the Control and NoSurf (Figure 3b) in particular at the shallow and middle depths, indicating that the CHT process within the soils influences the soil thermal regime as well, although its effect is not as strong as those due to infiltration from the surface .

During melting periods in spring when air temperature is higher than soil temperature, meltwater infiltrates into the soils along with warmer water temperature and warms the soils, as manifested by 315 higher simulated soil temperatures in Control than either NoSurf or NoConv. However, in Figure 3, we also found the moments that simulated temperature under the Control scenario is lower than that under NoSurf and NoConv. It indicates the existence of a cooling effect CHT, although such cooling effect is markedly weaker than the heating effect. The culprit is the direction of convective flux as well as the



temperature difference between soil layers. If the fluxes move from a higher temperature layer to a lower
320 temperature layer, the low-temperature layer is heated up, and vice versa. It is interesting that in
comparison to Control-NoSurf (Figure 3c), more negative differences (in blue) exist in Control-NoConv
(Figure 3c). It implies the liquid migration within the soils is more frequent to exert cooling effects on
the thermal regimes than the surface infiltration.



325 **Figure 3** Simulated hourly soil temperature profiles under the Control scenario (a), and the differences in
soil temperature between the scenarios: Control-NoSurf (b) and Control-NoConv (c). Control, NoSurf and
NoConv represent a full, partial and completely-absent consideration of convective heat transfer in the SHAW
model, respectively. NoSurf removes convective heat transfer due to infiltration and NoConv completely
removes convective heat transfer from the model.

330

The UWC differences between the scenarios (Figure 4) are similar in both space and time with the soil
temperature differences. The effects occurred mainly in thawing periods, and were weakened with
increasing depth. In the late spring of 2009, the patterns of UWC differences remarkably differ from
those in the same months of the neighboring years (Figure 4b, c). The 2009 differences are restricted to
335 the shallow depths while in the adjacent years the differences pervade the most soil depths. The 2009



340 pattern of UWC is also different from the pattern of soil temperature in the same year (Figure 3b, c) where no occurrences of temperature difference are observed in the shallow depths. It implies due to relatively smaller water migration magnitudes during the melting period of this year compared to the neighbouring years, CHT promotes only the phase change, producing more liquid water from ice, but is unable to perceptibly increase soil temperature.

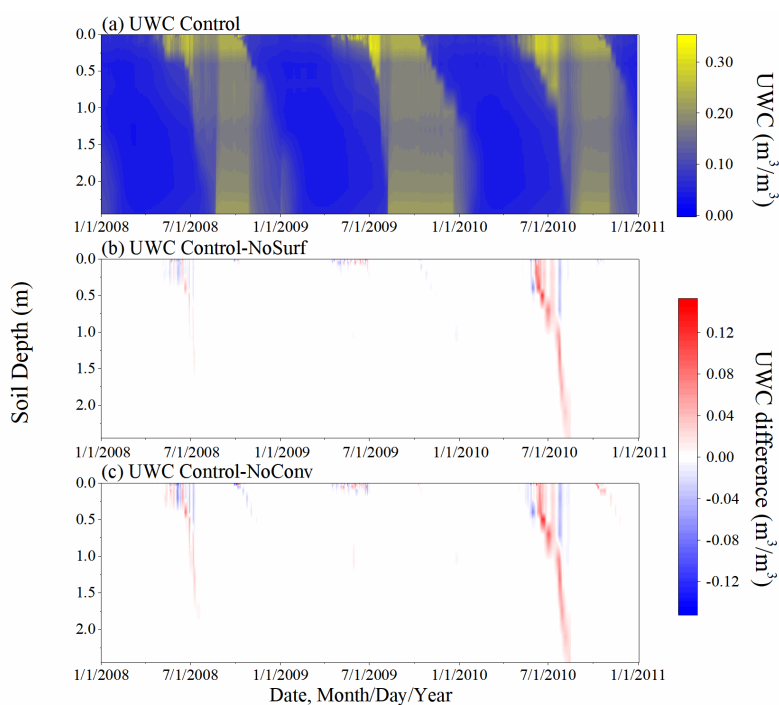


Figure 4 Simulated hourly soil unfrozen water content (UWC) profiles under the Control scenario (a), and the differences in UWC between the scenarios: Control-NoSurf (b) and Control-NoConv (c).

3.3 Stratified effects of convective heat transfer

345 3.3.1 Shallow depths

By contrasting the results in the shallow depths of NoSurf and NoConv with Control, the effects of CHT were quantified as shown in Figure 5 and Figure 6. The patterns are similar for all shallow depths, so the depth of 0.05 m was selected as a representative. Generally, effects on the thermal regime in the shallow depths are strong as quantified by the soil temperature differences in the 0.05 m depth during 2008 and 350 2010 obtained from both Control-NoSurf and Control-NoConv (Figure 5a and Figure 6a). In the figures,



positive differences in soil temperature represent heating effects of CHT on the shallow depths, while negative values represent cooling effects. The convective heat estimated in Control acts as an extra heat source that warms up the soils, increasing the soil temperature by as much as 10 °C during spring melting periods in addition to accomplishing phase changes from ice to water, as compared with the results of
355 NoSurf and NoConv. Meanwhile, in Figure 5 and Figure 6, soil temperatures simulated under Control (black dash line in Figure 5c and Figure 6c) had raised above 0 °C at the last stage of melting, whereas the temperatures of NoSurf (blue line in Figure 5c) and NoConv (red line in Figure 6c) still remained at 0 °C. It suggests the ending of zero-curtain effect was advanced for several days due to the heating effect of CHT as simulated in Control in comparison to those in NoSurf with partial presence of convective
360 heat considered and NoConv with no convective heat considered.

Apart from the heating effect imposed, an opposite, cooling effect is observed in the shallow depths, indicated as negative differences in Figure 5a and Figure 6a. It reduced soil temperature by up to -5 °C in some specific durations during the melting period in spring and the freezing period in fall by contrasting the results of Control with NoSurf and NoConv. The cooling effect is mainly related to
365 upward water flow driven by hydraulic gradient in the melting periods and negative temperature differences between the low-temperature surface and the high-temperature soils when infiltration happens.

We already draw the finding from Figure 3 that more cooling effects were introduced by the convective processes within the soils than those due to infiltration. It becomes more obvious by comparing Figure
370 6a showing Control-NoConv with Figure 5a showing Control-NoSurf.. Moreover, Figure 6a contains more nonzero values than Figure 5a. It is reasonable because the results of Control-NoConv include the entire effects of CHT, whereas Control-NoSurf includes only a partial portion relating to surface infiltration.

The pikes of liquid water migration within the 0.05 m layer, as shown in Figure 5b and Figure 6b, where
375 positive values indicate downward flows and negative for upward, highly agree the occurrences of CHT (Figure 5a and Figure 6a). During the zero-curtain durations in 2008 and 2010, the soils had undergone repeating freeze and thaw. Liquid water migration became more frequent after the soils had completely thawed and soil moisture content began to increase. At that time, CHT became more active in this depth.



It was not the same in 2009 spring, when a prolonged zero-curtain period was simulated and water flow
380 in soils was suppressed. As a result, marginal effects of CHT were observed over this period.

In the summer when the zero-curtain has completely ended, the soils held a relatively stable soil moisture
content. In this period, liquid water mainly percolated through the soils at a slow rate. The rate could
sometimes reach half of the peak liquid flux in spring melting at its maximum. However, only a small
increase of about 0.1 to 0.5 °C in soil temperature, or approximately 10% of the heating effect in spring,
385 could be caused by convective heat accompanying with water migration.

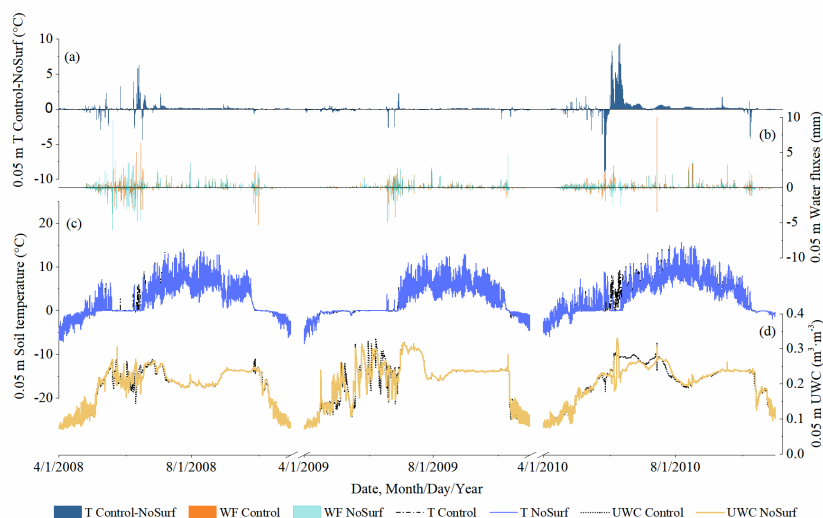
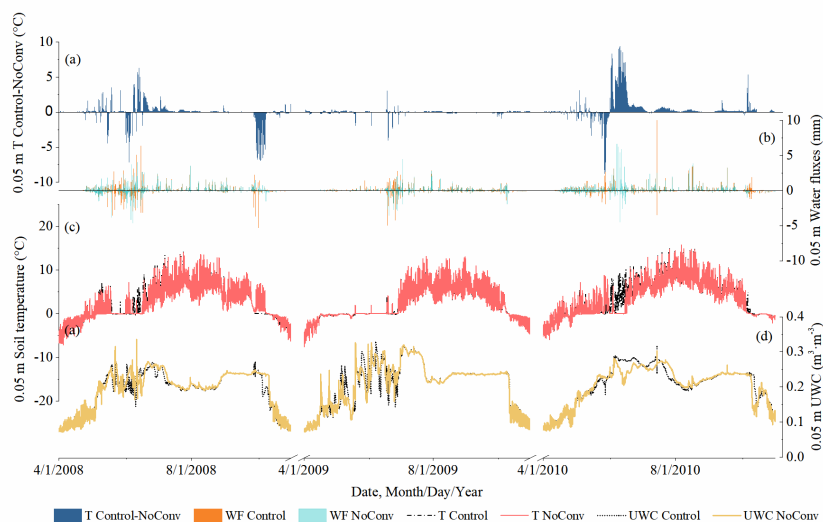


Figure 5 Soil temperature, water flux and UWC at the 0.05 m depth, as a representative of the shallow depths,
simulated under NoSurf and Control during the thawing periods of 2008-2010. From top to bottom are: (a)
the differences in soil temperature (T) between Control and NoSurf (Control-NoSurf), with positive values
390 indicating heating effects and negative values indicating cooling effects; (b) water fluxes (WF) simulated under
NoSurf and Control, in which positive value represents downward flow and negative for upward; (c) soil
temperatures and (d) UWCs simulated under NoSurf and Control.



395 **Figure 6** Soil temperature, water flux and UWC at the 0.05 m depth simulated under NoConv and Control during the thawing periods of 2008-2010. From top to bottom are: (a) the differences in soil temperature (T) between Control and NoConv (Control- NoConv) , with positive values indicating heating effects and negative values indicating cooling effects; (b) water fluxes (WF) simulated under NoConv and Control, in which positive value represents downward flow and negative for upward; (c) soil temperatures and (d) UWCs simulated under NoConv and Control.

400 **3.3.2 Middle depths**

Differing from the strong effects at the shallow depths, the effects of CHT on thermal and hydrological regimes at the middle depths of the active layer are not so much pronounced, as shown in Figure 7 and Figure 8 displaying the results at the depth of 1.05 m as a representative of the middle depths, due to inactive water migration occurring at those depths. Nevertheless, the characteristics of the occurrences appeared similar to those at the shallow depths in spite of weakened magnitudes. The temperatures at these depths were about 1 to 2 °C higher in the Control simulation than the NoSurf simulation sometime during the thawing periods. The comparison also show there was one day earlier in Control for the complete thaw in the active layer, because of the warming effect of convective heat penetrating from the surface downwards, which is present in the Control setup. The cooling effect imposed by convective heat was also found within the soil layers in certain periods. In these cases, the temperatures in NoConv surpassed those in Control by about 1 °C. It is primarily attributed to the joint effects of the weak

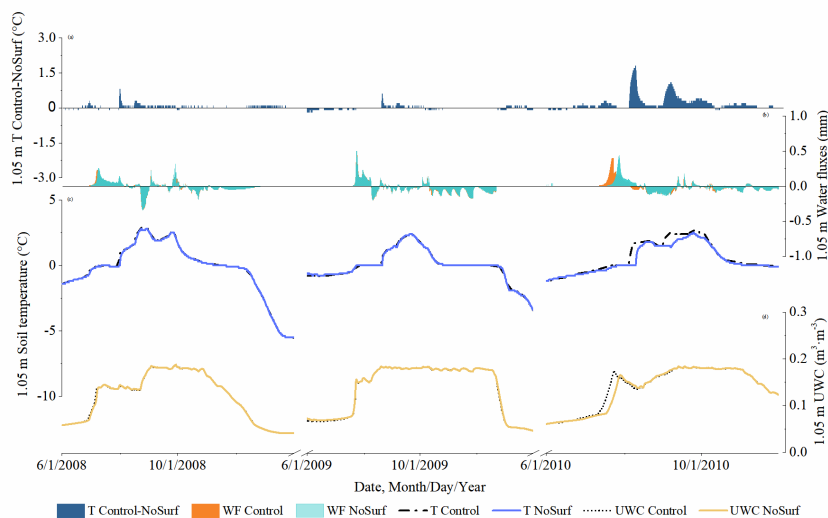
405

410



infiltration from the surface and the upward water fluxes within the middle depths that brought cooler water from the lower depth to the upper depth.

Another notable dissimilarity to the shallow depths is the apparent incoincidence between the occurrences of CHT and the peaks of water migration at the middle depths. When the vertical advection occurs within the middle depths, the small amount of inputting heat along with the advection can hardly satisfy the consumption of ongoing phase change, which requires a large amount of heat, and thus usually impossible to directly increase soil temperature of the lower layer. However, this process alters the thermal gradients of the soil column, which gradually influencing the total thermal regime. This is a delayed and slow responses, resulting in asynchronous occurrences of spikes in temperature and water fluxes as shown in Figure 7 and Figure 8.



425 **Figure 7** Soil temperature, water flux and UWC at the 1.05 m depth, as a representative of the middle depths, simulated under NoSurf and Control during the thawing periods of 2008-2010. The same notations as in **Figure 5** are applied.

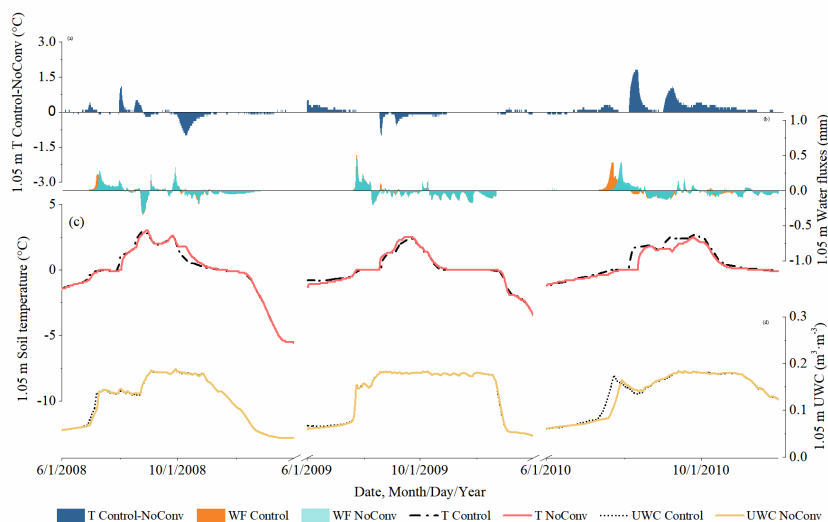
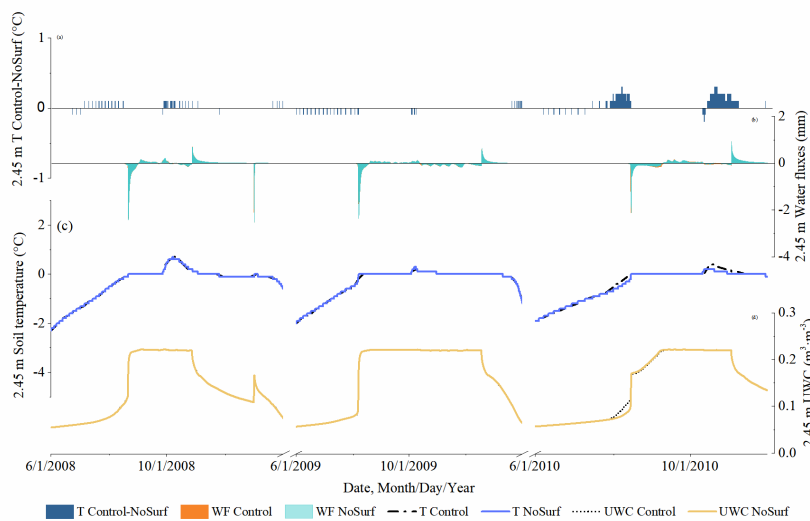


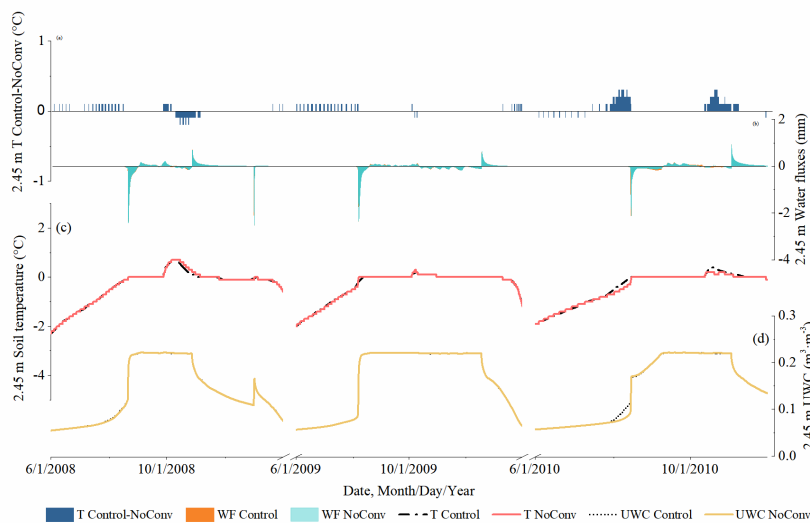
Figure 8 Soil temperature, water flux and UWC at the 1.05 m depth simulated under NoConv and Control during the thawing periods of 2008-2010. The same notations as in Figure 6 are applied.

430 3.3.3 Deep depths

The thermal impacts of CHT were minimal at the deep depths as shown in Figure 9a and Figure 10a. Accordingly, the water flow rarely occurred at the 2.45 m depth (Figure 9b and Figure 10b), with a frequency much less than that at the shallow and middle depths. The soil temperature in many thawing periods remained at zero degree (Figure 9c and Figure 10c). According to the study of Romanovsky and Osterkamp (2000), CHT associated with advection of unfrozen pore water no longer impacts soil temperature when the ambient soils hold a temperature close to the frozen point same as the migrating liquid. The existence of temperature gradient between depths is a prerequisite for inducing thermal impacts of CHT. In the deep depths, however, soil temperature slightly fluctuates throughout a year and only tiny differences in temperature from that of advective unfrozen water has produced. Therefore, some marginal temperature differences (less than 0.5 °C) were observed in this study by comparing NoSurf/NoConv with Control. It indicates the thermal effects of CHT are marginal in the deep depths of the active layer and usually can be ignored, although the vertical advection processes can be occasionally observed.



445 **Figure 9** Soil temperature, water flux and UWC at the 2.45 m depth, as a representative of the deep depths, simulated under NoSurf and Control during the thawing periods of 2008-2010. The same notations as in Figure 5 are applied.



450 **Figure 10** Soil temperature, water flux and UWC at the 2.45 m depth simulated under NoConv and Control during the thawing periods of 2008-2010. The same notations as in Figure 6 are applied.



4. Discussion

4.1 Twofold thermal impacts of convective heat transfer

This study has investigated two types of liquid CHT, i.e., the one due to infiltration from surface snow melt or rainfall and the other occurring within the soil column driven by hydraulic gradient, using a numerical modelling approach. During the thawing periods, soil temperature generally has a declining trend from the surface downward and along the depth. Thus, the infiltrative water moves downward with warmer temperature and imposes a heating effect on the soils passing through, likely to accelerate the process of phase change, especially in the later spring. This mechanism can explain some observations that sudden warming events occurred at certain depths during the spring melting periods as reported in the previous study (Hinkel et al., 2001).

However, CHT also probably produces a cooling effect within the active layer. The actual role of CHT at specific time depends on the direction of the liquid flow and the temperature difference along the flow path at that time. In the case that air temperature and surface temperature rapidly drop to below the subsurface soil temperature, the water flow from the ground surface to the soil layer may reduce soil temperature, as demonstrated in our contrasting experiments where soil temperature in Control, which is with full consideration of CHT, was simulated to be lower than that in NoSurf, which ignores infiltrative convective heat, at the shallow depths (0-0.2 m) in some periods. The other cause of cooling is related to upward water migration, such as return flow simulated in the SHAW model, in the thawing period, when the lower depth is colder than the upper depth in the soils. By contrasting Control-NoSurf with Control-NoConv, we found many cooling events occurring at the middle depths (0.4-1.3 m) within the soils and are associated with the upward water migration driven by hydraulic gradient, resulting in higher simulated soil temperature simulated in NoConv (which completely removes the CHT process) than in Control. Some previous studies (Gao et al., 2020; Li et al., 2016) has reported that the melting occurring at the permafrost table provides water supply to the upper depths. The consequent impacts on the thermal and hydrological regimes of the entire active layer caused by the upward liquid movement also have been reported (Chen et al., 2019; Cui et al., 2020). Our study strengthens those existing studies by quantifying and explaining such effects from a modelling perspective. In addition, Kurylyk et al. (2016) mentioned the potential thermal impact coming from lateral discharges in permafrost regions in spite of relatively



less magnitude. Unfortunately, it is not investigated in this study because the one-dimensional SHAW
480 model ignores lateral water migration from the perimeter into the soil column due to soil anisotropy, and
it may lead to some uncertainty regarding to the simulation of water flux within the active layer.

Summer rainfall is believed to have an important role in modulating the thermal regime in the active
layer(Wright et al., 2009; Zhang et al., 2021). Kane et al. estimated heat transfer due to the rainwater
infiltration into the shallow layer may be twice more than the conductive heat. Rachlewicz and
485 Szczuciński (2008)also postulated that non-conductive heat due to rainwater infiltration is particularly
important for the thermal regime in the upmost soil about 5 cm deep. However, this study shows the
effects of CHT due to rainfall in summer were much less in magnitude than in the spring melting periods
(Figure 5a). In Figure 5b, the downward water fluxes (shown as positive values) responded well to the
summer rainfalls in the near surface ground, whereas the impacts on soil temperature (Figure 5a) in this
490 depth induced by CHT are minimal. Those findings are not contradicted each other. The summer rainfall
has multifaceted non-conductive effects, including cooling the topsoil due to amplified
evapotranspiration from the ground surface, modifying the soil properties such as thermal capacity and
conductivity by adding more liquid water into the soils, rapidly transporting external heat to the soils
through percolation, and providing heat to the melting process occurring at the freeze-thaw front as a
495 heat source when additional liquid water accumulates above the front(Zhang et al., 2021). In this study,
hydraulic and hydrological functions of precipitation are the same in the scenarios, therefore, only the
effect of rapid transportation of external heat down to the soils are connected to the CHT process under
investigation, which was found to be of less importance among the multiple effects brought by the
summer rainfall.

500 4.2 Effects of soil moisture migration in late spring

In permafrost regions, soil moisture migration within the active layer is a major form to support CHT.
The liquid water migration at the shallow depths occurred most frequently during the spring melting
periods as simulated, transporting considerable heat to the low-depth soils and inducing remarkable
thermal impacts on soil temperature in line with these water migration events. Measurements of UWC at
505 some typical permafrost sites indicate that during late spring when ground ice melts, the UWC rapidly
rises to the highest before gradually dropping back to the field capacity till summer(Boike et al., 1998).



Before thaw begins, excessive ground ice accumulates at the shallow layers due to lowered soil permeability in the freezing process that inhibits the upper liquid water from percolating into the depth, and the presence of potential gradient between the freezing front that continues to move downward and the underlying unfrozen layer. The segregation potential of frozen soil drives the liquid flux moving upward to the front. As a consequence, the shallow frozen layers tend to hold excessive ice content much more than the liquid equivalent can be held (i.e. field capability) in the melting soil (Perfect and Williams, 1980; Chen, 1982). SHAW considers the decrease in permeability due to growth of soil ice, but ignores the mechanism of segregated ice. Despite this flaw, at the beginning of thaw, nearly saturated liquid water can be simulated and the portion beyond the field capacity moves downward or upward as return flow. It explains the formation of frequent and intense water migration occurring in the late spring, which makes strong CHT possible in those specific depths and periods.

4.3 Limitations

Existing observation-based studies indicate the unfrozen pore water can still migrate under the capillary force and van Der Waals force, even when the soil is completely frozen (Fisher et al., 2020; Kane and Stein, 1983). The SHAW model is in theory unable to simulate this process in the completely frozen periods. Therefore, the discrepancies in simulated soil temperature in January 2010 are actually linked to the extra snowmelt calculated as illustrated in Figure 2. Those snowmelt affects the temperature on the surface (0.0 m) and consequently creates a temperature gradient by which the thermal regime at the shallow depths is affected via conduction as depicted in Figure 3b and c.

The SHAW model assumes that the direction of vapor flux is the same with the liquid water and adopts a simplified consideration of air flow in the soils. It may lead to miscalculate the vapor convection. According to previous studies (Li et al., 2010; Yu et al., 2020), the evapotranspiration together with the CHT due to vapor flow plays an important role in the near surface soils in the thawing periods. Apart from the convective effect, air fluxes passing through the soils may also alter thermal properties such as freezing point (Ming et al., 2020) or infiltration rate (Prunty and Bell, 2016). Such oversimplified assumptions in SHAW are possible factors contributing to a prolonged zero-curtain period in the simulation. In addition, SHAW permits long term coexistence of mixed solid-liquid state in the physics. In reality, the inhomogeneity in soil property and the interference of surrounding conditions usually make



535 it hard to maintain a long-term coexistence (Akyurt et al., 2002). In wake of the weaknesses in physics
implemented in the SHAW model, we focused on investigating the role of CHT due to infiltration and
liquid migration through the soils while maintaining the rest all the same in the scenarios for comparison.
By subtracting the results from the two scenarios with modified models from that of the control scenario
with the original model, the uncertainties associated with those weaknesses will be reduced to the greatest
540 extent and the findings are thus more reliable.

The SHAW model implements a special Newton-Raphson procedure to solve energy and mass balance
equations, in which automated division of finer time steps is invoked if the solution is not satisfactory.
In this process of iterating over finer time steps, high quality upper and lower boundaries are necessary
to maintain a high simulation accuracy (Chen et al., 2019; Flerchinger, 1991). However, as a byproduct
545 of this process, the importance of conduction resulting from the boundaries are amplified as the extra
iterations proceed and as a consequent, the effects of nonconductive heat transfer are likely to be
underestimated.

5. Conclusions

This study utilized SHAW model in a typical permafrost distributed area, the Tanggula site at the eastern
550 Qinghai-Tibetan Plateau, to explore and quantify the effects of liquid CHT on the active layer thermal
regime. By modifying the SHAW model, we set up a control experiment consisting of three scenarios
representing the cases with full, partial or no consideration of CHT in the SHAW model. The following
conclusions have been concluded:

(1) The SHAW model demonstrated good performance in simulating soil temperature and moisture
555 dynamics in the active layer. The NSE for the simulated temperature and moisture content in most of soil
layers exceed, respectively, 0.7 and 0.45 in both calibration and validation periods.

(2) Liquid CHF is most likely to occur during the later spring and summer on the QTP when the frozen
ground at the shallow (0-0.2 m) and middle (0.4-1.3 m) depths had completely thawed. The infiltrative
snowmelt and precipitation from ground surface into the active layer is the major form of CHT in
560 permafrost regions. Only minimal influences of convective heat were found in freezing periods.

(3) In the shallow depth (0.0 m to 0.4 m), CHT is more active in the spring melt period than in summer.
During the melting period in spring, the differences in soil temperature simulated with or without



565 considering convective heat transfer had a large range from -5 to 10 °C, whereas in summer, the differences were around 0.5 °C, 10% of that in spring, despite of comparable magnitude of the peak convection flux to that in spring. In the middle layer (0.4-1.3 m), much less impacts of CHT and no obvious seasonal variations were simulated due to the weakened convective flow, causing a much smaller effect in altering soil temperature by only about -1.0 to 1.5 °C.

570 (4) CHT has proven twofold thermal impacts on active layer temperature, although the heating effect dominates in an annual freeze-thaw cycle on the QTP. During frozen ground melting in spring, soil temperature was simulated to be at most 10.0 °C higher in the shallow depth and 1.5 °C in the middle depth with infiltrative convective heat considered than no infiltrative heat transfer considered, and the closing dates of zero-curtain were considerably advanced. Meanwhile, the opposite cooling effect due to presence of upward liquid fluxes and thermal differences between the soil layers can lower the simulated soil temperature by up to -5 °C in shallow layer during some periods of spring, as indicated by comparing the simulation with CHT considered to the one with no CHT considered. By contrasting the scenario ignoring CHT due to infiltration with the scenario ignoring complete CHT, the liquid CHT processes within the soils led to a reduction of -1 °C in temperature in the middle soil layer.

Code and data availability

580 The source codes of Simultaneous Heat and Water (SHAW) Model can be freely downloaded from USDA Agricultural Research Service (<https://www.ars.usda.gov/pacific-west-area/boise-id/northwest-watershed-research-center/docs/shaw-model/>). The meteorological driving data and measured temperature and moisture data of active layer at the Tanggula site under study can be downloaded from National Cryosphere Desert Data Center (<https://www.ncdc.ac.cn/portal/>). The modified codes and simulation results of this study are openly available at <https://doi.org/10.6084/m9.figshare.14827959>.

585

Author contributions

Z.N. conceived and conceptualized the idea; Y.Z. and Z.N. developed the methodology; Y.Z., Z.N. and H.J. performed the analyses; Z.N. and L.Z. acquired the funding and provided the resources; Z.N.



supervised the study; Y. Z. wrote the draft version; Z.N., Y. Z., H.J. and L.Z. reviewed and edited the
590 writing.

Competing interests

The authors declare that there is no conflict of interest.

Acknowledgements

This study was supported by National Natural Science Foundation of China under the grants 41931180
595 and 41971074. The authors thank the National Cryosphere and Desert Data Center for providing data
and USDA Agricultural Research Service for providing the model.

References

- Akyurt, M., Zaki, G., Habeebullah, B.: Freezing Phenomena in Ice – Water Systems, *Energy Conversion*
600 and Management, 43, 1773-1789, [https://doi.org/10.1016/s0196-8904\(01\)00129-7](https://doi.org/10.1016/s0196-8904(01)00129-7), 2002.
- Biskaborn, B. K., Smith, S. L., Noetzli, J., Matthes, H., Vieira, G., Streletskiy, D. A., Schoeneich, P.,
Romanovsky, V. E., Lewkowicz, A. G., Abramov, A., Allard, M., Boike, J., Cable, W. L.,
Christiansen, H. H., Delaloye, R., Diekmann, B., Drozdov, D., Etzelmüller, B., Grosse, G.,
Guglielmin, M., Ingeman-Nielsen, T., Isaksen, K., Ishikawa, M., Johansson, M., Johannsson,
605 H., Joo, A., Kaverin, D., Kholodov, A., Konstantinov, P., Kröger, T., Lambiel, C., Lanckman,
J., Luo, D., Malkova, G., Meiklejohn, I., Moskalenko, N., Oliva, M., Phillips, M., Ramos, M.,
Sannel, A. B. K., Sergeev, D., Seybold, C., Skryabin, P., Vasiliev, A., Wu, Q., Yoshikawa, K.,
Zheleznyak, M., Lantuit, H.: Permafrost is Warming at a Global Scale, *Nature Communications*,
10, <https://doi.org/10.1038/s41467-018-08240-4>, 2019.
- 610 Boike, J., Hagedorn, B., Roth, K.: Heat and Water Transfer Processes in Permafrost-Affected Soils: A



- Review of Field and Modeling Based Studies for the Arctic and Antarctic, 2008.
- Boike, J., Roth, K., Overduin, P. P.: Thermal and Hydrologic Dynamics of the Active Layer at a Continuous Permafrost Site (Taymyr Peninsula, Siberia), *Water Resources Research*, 34, 355-363, <https://doi.org/10.1029/97WR03498>, 1998.
- 615 Cahill, A. T., Parlange, M. B.: On Water Vapor Transport in Field Soils, *Water Resources Research*, 34, 731-739, <https://doi.org/10.1029/97WR03756>, 1998.
- Chen, J., Gao, X., Zheng, X., Miao, C., Zhang, Y., Du, Q., Xu, Y.: Simulation of Soil Freezing and Thawing for Different Groundwater Table Depths, *Vadose Zone Journal*, 18, <https://doi.org/10.2136/vzj2018.08.0157>, 2019.
- 620 Cheng, G.: Influences of Local Factors On Permafrost Occurrence and their Implications for Qinghai-Xizang Railway Design, *Science in China Series D: Earth Sciences*, 47, 704-709, 2004.
- Cheng, G., Sun, Z., Niu, F.: Application of the Roadbed Cooling Approach in Qinghai - Tibet Railway Engineering, *Cold Regions Science and Technology*, 53, 241-258, <https://doi.org/10.1016/j.coldregions.2007.02.006>, 2008.
- 625 Cheng, G., Wu, T.: Responses of Permafrost to Climate Change and their Environmental Significance, Qinghai-Tibet Plateau, *Journal of Geophysical Research*, 112, <https://doi.org/10.1029/2006JF000631>, 2007.
- Cui, L., Zhu, Y., Zhao, T., Ye, M., Yang, J., Wu, J.: Evaluation of Upward Flow of Groundwater to Freezing Soils and Rational Per-Freezing Water Table Depth in Agricultural Areas, *Journal of Hydrology*, 585, 124825, <https://doi.org/10.1016/j.jhydrol.2020.124825>, 2020.
- 630 Fisher, D. A., Lacelle, D., Pollard, W.: A Model of Unfrozen Water Content and its Transport in Icy Permafrost Soils: Effects On Ground Ice Content and Permafrost Stability, *Permafrost and*



- Periglacial Processes, 31, 184-199, <https://doi.org/10.1002/ppp.2031>, 2020.
- Flerchinger, G. N.: Sensitivity of Soil Freezing Simulated by the Shaw Model, Transactions of the Asae,
635 34, 2381-2389, <https://doi.org/10.13031/2013.31883>, 1991.
- Flerchinger, G. N., Baker, J. M., Spaans, E.: A Test of the Radiative Energy Balance of the Shaw Model
for Snowcover, Hydrological Processes, 10, 1359-1367, [https://doi.org/10.1002/\(SICI\)1099-1085\(199610\)10:10<1359::AID-HYP466>3.0.CO;2-N](https://doi.org/10.1002/(SICI)1099-1085(199610)10:10<1359::AID-HYP466>3.0.CO;2-N), 1996.
- Flerchinger, G. N., Pierson, F. B.: Modelling Plant Canopy Effects On Variability of Soil Temperature
640 and Water: Model Calibration and Validation, Journal of Arid Environments, 35, 641-653,
<https://doi.org/10.1006/jare.1995.0167>, 1997.
- Flerchinger, G. N., Saxton, K. E.: Simultaneous Heat and Water Model of a Freezing Snow-Residue-Soil
System I. Theory and Development, Transactions of the Asae, 32, 565-571,
<https://doi.org/10.13031/2013.31040>, 1989a.
- 645 Flerchinger, G. N., Saxton, K. E.: Simultaneous Heat and Water Model of a Freezing Snow-Residue-Soil
System II. Field Verification, Transactions of the Asae, 32, 573-576,
<https://doi.org/10.13031/2013.31041>, 1989b.
- Gao, J., Xie, Z., Wang, A., Liu, S., Zeng, Y., Liu, B., Li, R., Jia, B., Qin, P., Xie, J.: A New Frozen Soil
Parameterization Including Frost and Thaw Fronts in the Community Land Model, Journal of
650 Advances in Modeling Earth Systems, 11, 659-679, <https://doi.org/10.1029/2018MS001399>,
2019.
- Gao, T., Liu, J., Zhang, T., Kang, S., Liu, C., Wang, S., Sillanpää, M., Zhang, Y.: Estimating Interaction
Between Surface Water and Groundwater in a Permafrost Region of the Northern Tibetan
Plateau Using Heat Tracing Method, Sciences in Cold and Arid Regions, 12, 71-82,



- 655 <https://doi.org/10.3724/SP.J.1226.2020.00071>, 2020.
- Guo, D., Wang, H.: Simulation of Permafrost and Seasonally Frozen Ground Conditions On the Tibetan Plateau, 1981-2010, *Journal of Geophysical Research: Atmospheres*, 118, 5216-5230, <https://doi.org/10.1002/jgrd.50457>, 2013.
- Halliwel, D. H., Rouse, W. R.: Soil Heat Flux in Permafrost: Characteristics and Accuracy of Measurement, *Journal of Climatology*, 7, 571-584, <https://doi.org/10.1002/joc.3370070605>, 660 1987.
- Hansson, K., Šimůnek, J., Mizoguchi, M., Lundin, L., van Genuchten, M. T.: Water Flow and Heat Transport in Frozen Soil: Numerical Solution and Freeze-Thaw Applications, *Vadose Zone Journal*, 3, 693-704, <https://doi.org/10.2136/vzj2004.0693>, 2004.
- 665 Hasler, A., Talzi, I., Beutel, J., Tschudin, C., Gruber, S.: Wireless Sensor Networks in Permafrost Research: Concept, Requirements, Implementation, and Challenges, in: 9th International Conference on Permafrost, Fairbanks, Alaska, 29 June 2008 - 3 July 2008, 669-674, <https://doi.org/10.5167/uzh-3095>, 2008.
- Hinkel, K. M., Outcalt, S. I., Taylor, A. E.: Seasonal Patterns of Coupled Flow in the Active Layer at 670 Three Sites in Northwest North America, *Canadian Journal of Earth Sciences*, 34, 667-678, <https://doi.org/10.1139/e17-053>, 1997.
- Hinkel, K. M., Paetzold, F., Nelson, F. E., Bockheim, J. G.: Patterns of Soil Temperature and Moisture in the Active Layer and Upper Permafrost at Barrow, Alaska: 1993 - 1999, *Global and Planetary Change*, 29, 293-309, [https://doi.org/10.1016/S0921-8181\(01\)00096-0](https://doi.org/10.1016/S0921-8181(01)00096-0), 2001.
- 675 Huang, M., Gallichand, J.: Use of the Shaw Model to Assess Soil Water Recovery After Apple Trees in the Gully Region of the Loess Plateau, China, *Agricultural Water Management*, 85, 67-76,



- <https://doi.org/10.1016/j.agwat.2006.03.009>, 2006.
- Jiang, H., Zhang, W., Yi, Y., Yang, K., Li, G., Wang, G.: The Impacts of Soil Freeze/Thaw Dynamics
On Soil Water Transfer and Spring Phenology in the Tibetan Plateau, Arctic, Antarctic, and
680 Alpine Research, 50, e1439155, <https://doi.org/10.1080/15230430.2018.1439155>, 2018.
- Jin, H., He, R., Cheng, G., Wu, Q., Wang, S., Lü, L., Chang, X.: Changes in Frozen Ground in the Source
Area of the Yellow River On the Qinghai – Tibet Plateau, China, and their Eco-Environmental
Impacts, Environmental Research Letters, 4, 45206, <https://doi.org/10.1088/1748-9326/4/4/045206>, 2009.
- 685 Jorgenson, M. T., Racine, C. H., Walters, J. C., Osterkamp, T. E.: Permafrost Degradation and Ecological
Changes Associated with a Warming climate in Central Alaska, Climate Change, 48, 551-579,
<https://doi.org/10.1023/A:1005667424292>, 2001.
- Kahimba, F. C., Ranjan, R. S., Mann, D. D.: Modeling Soil Temperature, Frost Depth, and Soil Moisture
Redistribution in Seasonally Frozen Agricultural Soils, Applied Engineering in Agriculture, 25,
690 871-882, <https://doi.org/10.13031/2013.29237>, 2009.
- Kane, D. L., Hinkel, K. M., Goering, D. J., Hinzman, L. D., Outcalt, S. I.: Non-Conductive Heat Transfer
Associated with Frozen Soils, Global and Planetary Change, 29, 275-292,
[https://doi.org/10.1016/S0921-8181\(01\)00095-9](https://doi.org/10.1016/S0921-8181(01)00095-9), 2001.
- Kane, D. L., Hinzman, L. D., Zarling, J. P.: Thermal Response of the Active Layer to Climatic Warming
695 in a Permafrost Environment, Cold Regions Science and Technology, 19, 111-122,
[https://doi.org/10.1016/0165-232X\(91\)90002-X](https://doi.org/10.1016/0165-232X(91)90002-X), 1991.
- Kane, D. L., Stein, J.: Water Movement Into Seasonally Frozen Soils, Water Resources Research, 19,
1547-1557, <https://doi.org/10.1029/WR019i006p01547>, 1983.



- 700 Kurylyk, B. L., Hayashi, M., Quinton, W. L., McKenzie, J. M., Voss, C. I.: Influence of Vertical and
Lateral Heat Transfer On Permafrost Thaw, Peatland Landscape Transition, and Groundwater
Flow, *Water Resources Research*, 52, 1286-1305, <https://doi.org/10.1002/2015WR018057>,
2016.
- Li, Q., Sun, S., Xue, Y.: Analyses and Development of a Hierarchy of Frozen Soil Models for Cold
Region Study, *Journal of Geophysical Research*, 115, <https://doi.org/10.1029/2009JD012530>,
705 2010.
- Li, Z., Feng, Q., Wang, Q. J., Yong, S., Cheng, A., Li, J.: Contribution From Frozen Soil Meltwater to
Runoff in an in-Land River Basin Under Water Scarcity by Isotopic Tracing in Northwestern
China, *Global and Planetary Change*, 136, 41-51,
<https://doi.org/10.1016/j.gloplacha.2015.12.002>, 2016.
- 710 Link, T. E., Flerchinger, G. N., Unsworth, M., Marks, D.: Simulation of Water and Energy Fluxes in an
Old-Growth Seasonal Temperate Rain Forest Using the Simultaneous Heat and Water (Shaw)
Model, *Journal of Hydrometeorology*, 5, 443-457, [https://doi.org/10.1175/1525-7541\(2004\)005<0443:SOWAEF>2.0.CO;2](https://doi.org/10.1175/1525-7541(2004)005<0443:SOWAEF>2.0.CO;2), 2004.
- Luethi, R., Phillips, M., Lehning, M.: Estimating Non-Conductive Heat Flow Leading to Intra-
715 Permafrost Talik Formation at the Ritigraben Rock Glacier (Western Swiss Alps), *Permafrost
and Periglacial Processes*, 28, 183-194, <https://doi.org/10.1002/ppp.1911>, 2017.
- Ming, F., Li, D. Q., Liu, Y. H.: A Predictive Model of Unfrozen Water Content Including the Influence
of Pressure, Permafrost and Periglacial Processes, 31, 213-222,
<https://doi.org/10.1002/ppp.2037>, 2020.
- 720 Orgogozo, L., Prokushkin, A. S., Pokrovsky, O. S., Grenier, C., Quintard, M., Viers, J., Audry, S.: Water



- and Energy Transfer Modeling in a Permafrost-Dominated, Forested Catchment of Central
Siberia: The Key Role of Rooting Depth, Permafrost and Periglacial Processes, 30, 75-89,
<https://doi.org/10.1002/ppp.1995>, 2019.
- Outcalt, S. I., Nelson, F. E., Hinkel, K. M.: The Zero-Curtain Effect: Heat and Mass Transfer Across an
725 Isothermal Region in Freezing Soil, *Water Resources Research*, 26, 1509-1516,
<https://doi.org/10.1029/WR026i007p01509>, 1990.
- Perfect, E., Williams, P. J.: Thermally Induced Water Migration in Frozen Soils, *Cold Regions Science
and Technology*, 3, 101-109, [https://doi.org/10.1016/0165-232X\(80\)90015-4](https://doi.org/10.1016/0165-232X(80)90015-4), 1980.
- Pogliotti, P., Cremonese, E., Morra Di Cella, U., Gruber, S., Giardino, M.: Thermal Diffusivity
730 Variability in Alpine Permafrost Rock Walls, in: 9th International Conference on Permafrost,
Fairbanks, US., Institute of Northern Engineering, University of Alaska, Fairbanks, US., 2008.
- Prunty, L., Bell, J.: Infiltration Rate Vs. Gas Composition and Pressure in Soil Columns, *Soil Science
Society of America Journal*, 71, 1473-1475, <https://doi.org/10.2136/sssaj2007.0072N>, 2016.
- Putkonen, J.: Soil Thermal Processes and Heat Transfer Processes Near Ny-Ålesund, Northwestern
735 Spitsbergen, Svalbard, *Polar Research*, 17, 165-179, <https://doi.org/10.3402/polar.v17i2.6617>,
1998.
- Qi, J., Yao, X., Yu, F.: Consolidation of Thawing Permafrost Considering Phase Change, *Ksce Journal
of Civil Engineering*, 17, 1293-1301, <https://doi.org/10.1007/s12205-013-0240-1>, 2013.
- Rachlewicz, G., Szczuciński, W.: Changes in Thermal Structure of Permafrost Active Layer in a Dry
740 Polar Climate, Petuniabukta, Svalbard, *Polish Polar Research*, 29, 261-278, 2008.
- Riseborough, D. W.: Soil Latent Heat as a Filter of the Climate Signal in Permafrost, in: *Proceedings of
the Fifth Canadian Permafrost Conference, Collect, Nordicana*, 199-205, 1990.



- Romanovsky, V. E., Osterkamp, T. E.: Effects of Unfrozen Water On Heat and Mass Transport Processes in the Active Layer and Permafrost, *Permafrost and Periglacial Processes*, 11, 219-239, 2000.
- 745 Roth, K., Boike, J.: Quantifying the Thermal Dynamics of a Permafrost Site Near Ny-Alesund, Svalbard, *Water Resources Research*, 37, 2901-2914, [https://doi.org/10.1002/1099-1530\(200007/09\)11:3<219::AID-PPP352>3.0.CO;2-7](https://doi.org/10.1002/1099-1530(200007/09)11:3<219::AID-PPP352>3.0.CO;2-7), 2001.
- Scherler, M., Hauck, C., Hoelzle, M., Stahli, M., Volksch, I.: Meltwater Infiltration Into the Frozen Active Layer at an Alpine Permafrost Site, *Permafrost and Periglacial Processes*, 21, 325-334, 750 <https://doi.org/10.1002/ppp.694>, 2011.
- Shen, M., Piao, S., Jeong, S., Zhou, L., Zeng, Z., Ciais, P., Chen, D., Huang, M., Jin, C., Li, L. Z. X., Li, Y., Myneni, R. B., Yang, K., Zhang, G., Zhang, Y., Yao, T.: Evaporative Cooling Over the Tibetan Plateau Induced by Vegetation Growth, *Proceedings of the National Academy of Sciences*, 112, 9299-9304, <https://doi.org/10.1073/pnas.1504418112>, 2015.
- 755 Stein, J., Kane, D. L.: Monitoring the Unfrozen Water Content of Soil and Snow Using Time Domain Reflectometry, *Water Resources Research*, 19, 1573-1584, <https://doi.org/10.1029/WR019i006p01573>, 1983.
- Tesi, T., Muschitiello, F., Smittenberg, R. H., Jakobsson, M., Vonk, J. E., Hill, P., Andersson, A., Kirchner, N., Noormets, R., Dudarev, O., Semiletov, I., Gustafsson, Ö.: Massive Remobilization 760 of Permafrost Carbon During Post-Glacial Warming, *Nature Communications*, 7, <https://doi.org/10.1038/ncomms13653>, 2016.
- van der Velde, R., Su, Z., Ek, M., Rodell, M., Ma, Y.: Influence of Thermodynamic Soil and Vegetation Parameterizations On the Simulation of Soil Temperature States and Surface Fluxes by the Noah Lsm Over a Tibetan Plateau Site, *Hydrology and Earth System Sciences Discussions*, 6, 455-



- 765 499, <https://doi.org/10.5194/hessd-6-455-2009>, 2009.
- Wei, Z., Jin, H., Zhang, J., Yu, S., Han, X., Ji, Y., He, R., Chang, X.: Prediction of Permafrost Changes in Northeastern China Under a Changing Climate, *Science China Earth Sciences*, 54, 924-935, <https://doi.org/10.1007/s11430-010-4109-6>, 2011.
- Wicky, J., Hauck, C.: Numerical Modelling of Convective Heat Transport by Air Flow in Permafrost Talus Slopes, *The Cryosphere*, 11, 1311-1325, <https://doi.org/10.5194/tc-11-1311-2017>, 2017.
- 770 Woo, M. K., Marsh, P., Pomeroy, J. W.: Snow, Frozen Soils and Permafrost Hydrology in Canada, 1995-1998, *Hydrological Processes*, 9, 1591-1611, [https://doi.org/10.1002/1099-1085\(20000630\)14:9<1591::AID-HYP78>3.0.CO;2-W](https://doi.org/10.1002/1099-1085(20000630)14:9<1591::AID-HYP78>3.0.CO;2-W), 2000.
- Wright, N., Hayashi, M., Quinton, W. L.: Spatial and Temporal Variations in Active Layer Thawing and their Implication On Runoff Generation in Peat-Covered Permafrost Terrain, *Water Resources Research*, 45, <https://doi.org/10.1029/2008WR006880>, 2009.
- 775 Wu, X., Nan, Z., Zhao, S., Zhao, L., Cheng, G.: Spatial Modeling of Permafrost Distribution and Properties On the Qinghai-Tibet Plateau, *Permafrost and Periglacial Processes*, 29, 86-99, <https://doi.org/10.1002/ppp.1971>, 2018.
- 780 Xiao, Y., Zhao, L., Dai, Y., Li, R., Pang, Q., Yao, J.: Representing Permafrost Properties in Colm for the Qinghai - Xizang (Tibetan) Plateau, *Cold Regions Science and Technology*, 87, 68-77, <https://doi.org/10.1016/j.coldregions.2012.12.004>, 2013.
- Yu, L., Zeng, Y., Su, Z.: Understanding the Mass, Momentum, and Energy Transfer in the Frozen Soil with Three Levels of Model Complexities, *Hydrology and Earth System Sciences*, 24, 4813-4830, <https://doi.org/10.5194/hess-24-4813-2020>, 2020.
- 785 Zhang, G., Nan, Z., Zhao, L., Liang, Y., Cheng, G.: Qinghai-Tibet Plateau Wetting Reduces Permafrost



- Thermal Responses to Climate Warming, *Earth and Planetary Science Letters*, 562, 116858,
<https://doi.org/10.1016/j.epsl.2021.116858>, 2021.
- Zhang, T., Barry, R. G., Knowles, K., Heginbottom, J. A., Brown, J.: Statistics and Characteristics of
790 Permafrost and Ground - Ice Distribution in the Northern Hemisphere, *Polar Geography*, 23,
132-154, <https://doi.org/10.1080/10889379909377670>, 1999.
- Zhang, Y., Carey, S. K., Quinton, W. L.: Evaluation of the Algorithms and Parameterizations for Ground
Thawing and Freezing Simulation in Permafrost Regions, *Journal of Geophysical Research*, 113,
<https://doi.org/10.1029/2007JD009343>, 2008.
- 795 Zhao, L., Wu, Q., Marchenko, S. S., Sharkhuu, N.: Thermal State of Permafrost and Active Layer in
Central Asia During the International Polar Year, *Permafrost and Periglacial Processes*, 21, 198-
207, <https://doi.org/10.1002/ppp.688>, 2010.
- Zuo, Y., Guo, Y., Song, C., Jin, S., Qiao, T.: Study On Soil Water and Heat Transport Characteristic
Responses to Land Use Change in Sanjiang Plain, *Sustainability*, 11, 157,
800 <https://doi.org/10.3390/su11010157>, 2019.
- Chen, G.: The formation process of the thick underground ice, *Scientia Sinica*, 281-288, 1982. (In
Chinese with English abstract)
- Liu, Y., Zhao, L., Li, R.: Simulation of the soil water-thermal features within the active layer in Tanggula
Region, Tibetan Plateau, by using SHAW model, *Journal of Glaciology and Geocryology*, 35,
805 280-290, 2013. (In Chinese with English abstract)